

GENETICS

Gene drive mosquitoes can aid malaria elimination by retarding *Plasmodium* sporogonic development

Astrid Hoermann^{1†}, Tibebe Habtewold^{1†}, Prashanth Selvaraj², Giuseppe Del Corsano¹, Paolo Capriotti¹, Maria Grazia Inghilterra¹, Temesgen M. Kebede¹, George K. Christophides^{1*}, Nikolai Windbichler^{1*}

Gene drives hold promise for the genetic control of malaria vectors. The development of vector population modification strategies hinges on the availability of effector mechanisms impeding parasite development in transgenic mosquitoes. We augmented a midgut gene of the malaria mosquito *Anopheles gambiae* to secrete two exogenous antimicrobial peptides, magainin 2 and melittin. This small genetic modification, capable of efficient nonautonomous gene drive, hampers oocyst development in both *Plasmodium falciparum* and *Plasmodium berghei*. It delays the release of infectious sporozoites, while it simultaneously reduces the life span of homozygous female transgenic mosquitoes. Modeling the spread of this modification using a large-scale agent-based model of malaria epidemiology reveals that it can break the cycle of disease transmission across a range of transmission intensities.

INTRODUCTION

Malaria remains one of the most devastating human diseases. A surge in insecticide-resistant mosquitoes and drug-resistant parasites has brought a decades-long period of progress in reducing cases and deaths to a standstill (1). Despite the availability of the first World Health Organization–approved malaria vaccine (2) the necessity to develop alternative intervention strategies remains pressing, particularly if malaria elimination is to remain the goal. Gene drive, based on the super-Mendelian spread of endonuclease genes, is a promising new control strategy that has been under development for over a decade (3). Suppressing mosquito populations by targeting female fertility has remained a prime application of gene drives, and to date, specific gene drives have been shown to eliminate caged mosquito populations (4–6). Gene drives for population replacement (or modification), designed to propagate antimalarial effector traits, have also seen notable development in the past years (7–9). To date, a range of antimalarial effectors and tissue-specific drivers have been tested in transgenic mosquitoes, and some of them have been shown to reduce *Plasmodium* infection prevalence or infection intensity (10–23). However, the pursuit of novel and effective mechanisms is ongoing, especially in *Anopheles gambiae* where effectors so far have shown only moderate reductions in parasite transmission (12, 15, 20–22).

Antimicrobial peptides (AMPs) from reptiles, plants, or insects have long been considered putative antimalarial effectors and have been tested in vitro and in vivo for their efficacy against different parasite life stages [for reviews, see (24–27); for other relevant studies, see (28, 29)]. Although AMPs are very diverse in sequence and structure, many are cationic and amphiphilic and thus tend to adhere to negatively charged microbial membranes and, to a much

lesser extent, to membranes of animal cells (30). Permeabilization mechanisms have been proposed, which rely on either pore formation or accumulation of peptides on the microbial surface, causing disruption in a detergent-like manner (31). A subset of AMPs has been suggested to act by mitochondrial uncoupling, interfering directly with mitochondria-dependent adenosine triphosphate (ATP) synthesis (32–34). Two such peptides, magainin 2, found within skin secretions of the African claw frog *Xenopus laevis*, and melittin, a primary toxin component of the European honey bee *Apis mellifera*, have been shown to both form pores on the microbial membrane (35, 36) and trigger uncoupling of mitochondrial respiration (37–40). Intrathoracic injection of magainin 2 into *Anopheles* mosquitoes has been demonstrated to cause *Plasmodium* oocyst degeneration and shrinkage and a consequent reduction in the number of sporozoites released (41), while a transmission blocking effect of magainin 2 has also been revealed when spiked into gametocytic blood at a 50 μ M concentration (29). Similarly, melittin has been shown to reduce the number and prevalence of *Plasmodium falciparum* oocysts in spike-in experiments at concentrations as low as 4 μ M (28, 29), while expression of melittin in transgenic *Anopheles stephensi* mosquitoes as a part of a multieffector transgene, additionally including the AMPs TP10, EPIP, Shiva1, and Scorpine, has led to a significant reduction in oocyst prevalence and infection intensity (23).

RESULTS

Here, we augmented two host genes of *A. gambiae* to coexpress magainin 2 and melittin following the previously described integral gene drive (IGD) paradigm (42). This allowed for minimal genetic modifications, capable of nonautonomous gene drive, to be introduced into the host gene loci, making full use of the gene regulatory regions for controlling tissue-specific expression of the AMPs. We used the previously evaluated *zinc carboxypeptidase A1* (*CP*; AGAP009593) or the AMP *gambicin 1* (*Gam1*; AGAP008645) as host genes for the exogenous AMP integration, respectively (Fig. 1A). The transcriptional profile of these genes was expected to drive expression of the

Copyright © 2022
The Authors, some
rights reserved;
exclusive licensee
American Association
for the Advancement
of Science. No claim to
original U.S. Government
Works. Distributed
under a Creative
Commons Attribution
License 4.0 (CC BY).

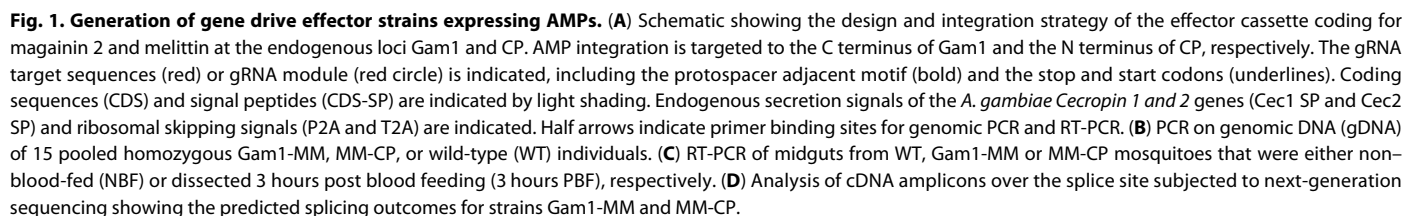
Downloaded from https://www.science.org at Universit degli Studi di Perugia on April 22, 2024

¹Department of Life Sciences, Imperial College London, London SW7 2AZ, UK.

²Institute for Disease Modeling, Bill and Melinda Gates Foundation, Seattle, WA 98109, USA.

*Corresponding author. Email: g.christophides@imperial.ac.uk (G.K.C.); n.windbichler@imperial.ac.uk (N.W.)

†These authors contributed equally to this work.



Next, we performed infection experiments with the *P. falciparum* NF54 strain to determine the effect of these modifications on parasite transmission (Fig. 2A). Both transgenic strains showed a significant reduction in the midgut oocyst loads on day 7 post infection (pi; Fig. 2B). While only a few oocysts of the MM-CP strain had the expected size, a closer examination of infected midguts revealed the presence of many smaller structures possibly representing stunted or aborted oocysts (Fig. 2C), prompting a more detailed investigation of this strain. We performed infections and quantified the number and diameter of all oocyst-like structures on days 7, 9, and 15 pi. Given that nutritional stress is a factor that recently emerged as causing stunting of oocysts (43, 44), a group of mosquitoes were provided a supplemental blood meal on day 4 pi. We found that the small oocyst-like structures were stunted oocysts that grew over time and that the supplemental blood meal further boosted their growth (Fig. 2D). Overall, oocysts infecting the MM-CP strain were significantly smaller than in the wild-type (WT) control by an average of 47.8, 41.1, and 59.8% on days 7, 9, and 15 pi, respectively (Fig. 2D). This was also the case for the cohort that received an additional blood meal, but the difference with WT controls decreased over time to 50.4, 24.9, and 18.6% on days 7, 9, and 15 pi, respectively. We repeated this experiment with the rodent parasite *Plasmodium berghei* to determine whether the observed infection phenotype would also occur with a different parasite species and under different environmental conditions. Using a GFP-labeled *P. berghei* ANKA 2.34 strain,

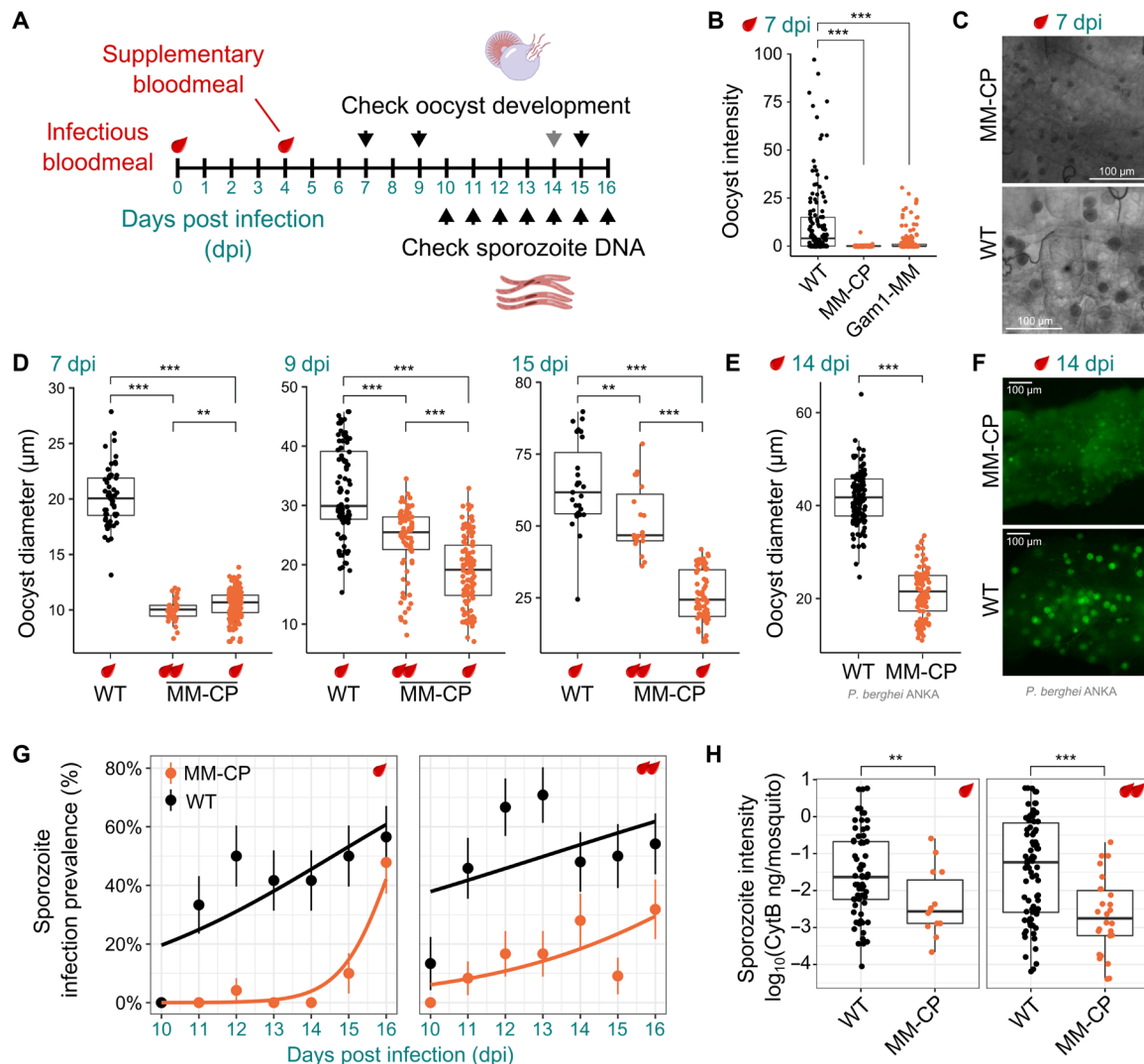


Fig. 2. *Plasmodium* infection experiments. (A) Schematic overview of *Plasmodium* infection experiments. (B) *P. falciparum* oocyst intensity 7 days pi (dpi) in midguts from WT, MM-CP and Gam1-MM mosquitoes dissected. Data from three biological replicates was pooled, and statistical analysis was performed using the Mann-Whitney test. (C) Bright-field images of midguts showing typical oocysts in WT and MM-CP mosquitoes at 7 dpi. (D) Quantification of *P. falciparum* oocyst diameter in WT and MM-CP mosquitoes 7, 9, and 15 dpi from three pooled biological replicates. Note that many oocysts in WT mosquitoes had ruptured on day 15 pi. Quantification of oocyst diameter (E) and fluorescent imaging (F) of oocysts in WT and MM-CP mosquitoes infected with *P. berghei* at 14 dpi. Sporozoite prevalence 10 to 16 dpi (G) and infection intensity across all days (H) was measured by qPCR of the *P. falciparum* Cyt-B gene in dissected heads and thoraces of individual MM-CP and WT mosquitoes (10 to 16 dpi). Only mosquitoes positive for oocyst DNA in the midgut were included in the analysis performed in two biological replicates. Statistical analysis in (D), (E), and (H) was performed by a *t* test assuming unequal variance. Statistical analysis in (G) was performed using a generalized linear model with a quasibinomial error structure where strain ($P = 8.35 \times 10^{-6}$) and dpi ($P = 7.15 \times 10^{-4}$) but not blood meal status ($P = 0.0894$) were found to be significant coefficients. In all panels, the provision of a supplemental blood meal 4 dpi is indicated by an additional blood drop. ** $P \leq 0.01$ and *** $P \leq 0.001$; ns, not significant.

fluorescent imaging revealed clearly stunted oocysts that, on day 14 pi, were about two times smaller than in the control (Fig. 2, E and F).

We reasoned that the detected retardation of oocyst development would, in turn, cause a delayed release of sporozoites into the mosquito hemocoel and subsequent infection of the salivary glands. To determine the sporozoite load over time, we determined the abundance of parasite DNA on days 10 to 16 pi by quantifying the *P. falciparum* cytochrome B (Cyt-B) gene in the head and thorax of single mosquitoes via quantitative PCR (qPCR), considering only mosquitoes that were positive for parasite DNA in the midgut. We found that sporozoite infection prevalence, i.e., the rate of head and

thorax samples with amplification above the amplification cycle threshold, was significantly reduced in MM-CP mosquitoes (Fig. 2G) when compared to WT (on average, by 77.9% across time points), with a significant number of positives detectable only on day 16. Although a supplemental blood meal accelerated sporozoite release in the MM-CP strain by 4 to 5 days (now detected on days 11 to 12 pi), overall sporozoite prevalence was still reduced significantly relative to the control group that had received a single blood meal by 67.8% on average. This suggested that sporozoite release in the MM-CP strain was delayed under both nutritional conditions. We also analyzed the relative parasite DNA content in positive samples as a proxy

for sporozoite numbers and found that these were significantly higher in WT compared to MM-CP mosquitoes both after a single (14.0-fold) or double (37.8-fold) blood meals (Fig. 2H). To rule out any founder effect in the homozygous MM-CP strain, we outcrossed MM-CP mosquitoes to mosquitoes of the *A. gambiae* Ifakara strain. After an F1 sibling cross, F2 mosquitoes were provided an infected blood meal and dissected on day 9 to assess the midgut oocyst size and be genotyped by PCR for the presence of the transgene. The results showed that the effect on parasite development was attributable to the presence of the transgene and that the developmental retardation of oocysts was reduced in hemizygous individuals (fig. S3).

Next, we measured fitness parameters of MM-CP mosquitoes. The number of eggs laid by blood-fed females (a measure of fecundity) and the number of eggs that hatched among those laid (a measure of fertility) were counted. The results showed a 14.1% difference in the number of eggs laid ($P = 0.0299$, two-sample t test assuming unequal variances) but unaffected larval hatching rates between the MM-CP and WT control mosquitoes (Fig. 3, A and B). Overall, larval output per female is shown in fig. S4. Pupal sex ratio (Fig. 3C) and pupation time did not significantly deviate between MM-CP and control mosquitoes (fig. S5). However, a significant effect on the life span of sugar-fed mosquitoes was detected for MM-CP females (median life span, 15 days) and, to a lesser extent, in males (23 days) compared to control females (26 days) and males (27 days; Fig. 3D). We repeated this experiment with females that were now also provided with regular blood meals. CP is only weakly expressed in the sugar-fed midgut, but baseline expression of the AMPs is nevertheless the most likely explanation for the observed fitness cost. In contrast,

CP is strongly induced following a blood feed, and thus, any effect of the transgene was expected to be elevated by the blood meals. As before, to blind the experiment and rule out that genetic background accounted for this effect, we first performed a backcross to the Ifakara strain and genotyped individual F2 mosquitoes that were raised as a mixed population at the end of the experiment. The results confirmed a significant life span reduction in homozygous MM-CP females under these conditions, but no significant effect was detected in hemizygous individuals compared to nontransgenic controls (Fig. 3E).

We performed transcriptomic analysis of dissected midguts before and 6 and 20 hours after blood feeding. We quantified the number of differentially expressed genes between MM-CP and control females and performed a gene ontology (GO) analysis to determine significantly enriched gene groups (table S1). The results indicated that genes involved in mitochondrial function and located at the inner mitochondrial membrane were disproportionately affected in MM-CP females, particularly after the blood meal (Fig. 3, F to H). Among most significant hits were genes encoding a member of the ubiquinone complex (AGAP003900), a mitochondrial H^+ adenosine triphosphatase (AGAP012818), an ATP synthase subunit (AGAP004788), and a protein belonging to a family of calcium channels (AGAP002578), which control the rate of mitochondrial ATP production. These findings offered a hypothesis that could explain the dual phenotype regarding parasite development and adult female life span. *Plasmodium* development in the mosquito is critically dependent on mitochondrial function including active respiration (45–48). Magainin 2 and melittin are known to trigger mitochondrial uncoupling and could, upon secretion into the midgut lumen, interfere with ATP

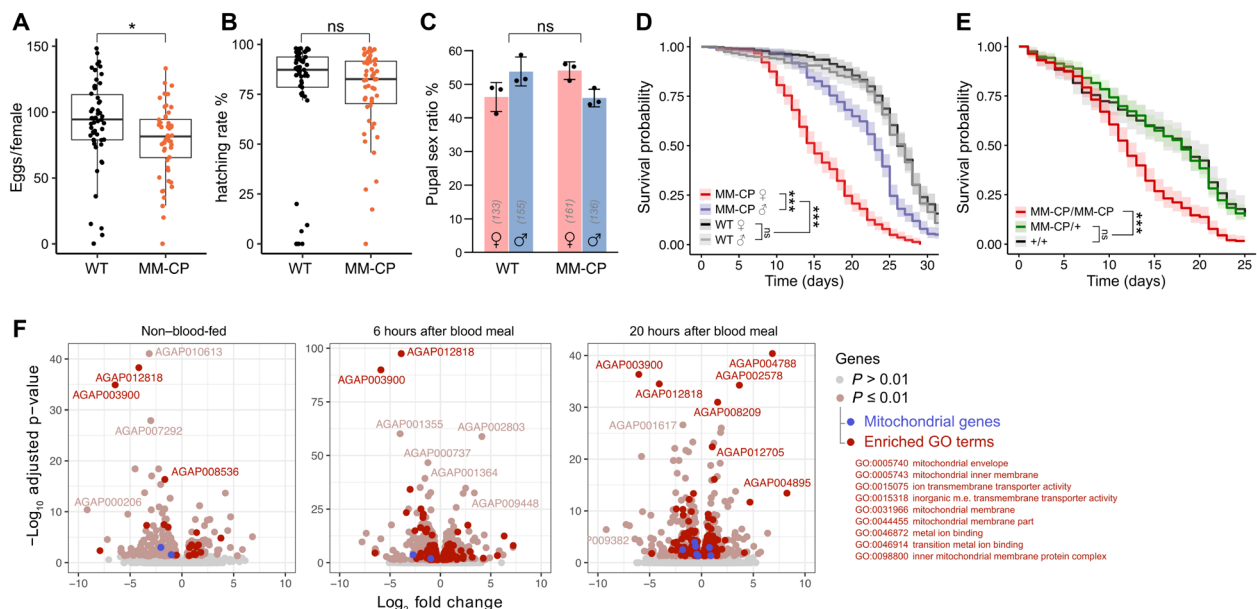


Fig. 3. Life history traits and midgut transcriptome of MM-CP mosquitoes. (A) Fecundity of individual homozygous MM-CP females compared to the WT and corresponding (B) larval hatching rates obtained during the first gonotrophic cycle. Data from three pooled biological replicates are shown. Statistical significance was determined by a t test assuming unequal variance. (C) Pupal sex ratios of MM-CP and WT strains analyzed using the chi-square test for equality. (D) Survival analysis of MM-CP and WT male and female mosquitoes maintained on sugar and (E) of F2 genotyped MM-CP female mosquitoes following backcrossing to the Ifakara strain, intercrossing of F1 mosquitoes, and provision of blood meals. Statistical significance was determined with a Mantel-Cox log rank test. Data from three biological replicates are pooled, and the mean and 95% confidence intervals are plotted. $*P \leq 0.05$ and $***P \leq 0.001$. (F) Volcano plots of an RNA sequencing (RNA-seq) experiment performed on midguts dissected before or 6 and 20 hours after blood meal. Differentially expressed genes between MM-CP and WT mosquitoes ($P \leq 0.01$) are indicated, and genes belonging to enriched GO groups are highlighted in red.

synthesis targeting the parasite mitochondrion. This effect would become apparent as the parasite transforms into the energy-demanding oocyst stage that undergoes several rounds of endomitosis and vegetative growth. As AMPs are unlikely to be able to access the oocyst, the effect would wear off with time and partly offset by supplemental blood meals. The AMPs, however, are likewise expected to affect the mosquito midgut mitochondria, affecting energy homeostasis and modulating life span. While further experiments are needed to untangle these effects, the most significant knowledge gap, when it comes to transmission blocking, is to what degree any effects observed with laboratory strains of *P. falciparum* would be reproducible in infections with genetically diverse parasites isolated from patient blood. The MM-CP strain is an excellent candidate to attempt to answer this question, as the transmission-blocking mechanism that we describe here appears to act across *Plasmodium* species. MM-CP is incapable of autonomous gene drive, unless it mates with a mosquito source of Cas9, and can thus be evaluated in an endemic setting under standard mosquito confinement protocols.

Last, we predicted how deployment of the MM-CP effector trait would modify malaria epidemiology using a mechanistic, agent-based model of *P. falciparum* transmission that includes vector life cycle and within-host parasite and immune dynamics. The model is based on the EMOD framework that has recently been updated to enable the simulation of gene drives (49). In our model, seasonality of rainfall and temperature ranges are characteristic of the Sahel for one representative year and were kept the same across transmission settings from year to year. Vector density was varied to match desired transmission intensity. There remain knowledge gaps that preclude a direct translation of experimental entomological or molecular data into epidemiological parameters, for example, linking the observed reduction in sporozoite DNA and its quantitative effect on onward

transmission. For the phenotypic effects, we thus estimated likely parameter value ranges (a 30 to 70% increase in time until sporozoites are released and a 40 to 100% reduction in infectious sporozoites) that we considered to be within physiologically plausible limits supported by our *in vivo* experiments. As a final parameter for the model, we experimentally determined the rate of nonautonomous gene drive of the MM-CP allele by pairing it with a source of Cas9, which resulted in high levels of homing of the transgene in both males and females: 96.01 and 98.91%, respectively (Fig. 4A). MM-CP, as a nonautonomous effector, could be flexibly deployed in conjunction with nondriving, self-limiting, or, as we assumed in our model, a fully autonomous Cas9 gene drive that is able to mobilize MM-CP (fig. S6). A single release of 1000 mosquitoes carrying the driver and MM-CP effector was conducted 6 months into the simulation, and simulations were run for a total of 6 years. We assumed that functional resistance (R1 alleles) at both loci would arise at 1% rate. We observed rapid propagation of MM-CP with all WT targets replaced by the end of year 2 of the simulations. Subsequently, MM-CP is gradually replaced by functional resistant alleles falling below 50% allele frequency by the end of year 4. We determined the probability of elimination by the last year of simulation, defined as the number of simulations per parameter set that have zero prevalence in the last year divided by the total number of simulations. Incidence reduction was evaluated for the duration of the simulation following gene drive releases compared to control scenarios with no releases. In a low transmission setting [annual entomological inoculation rate (EIR), ~15 infectious bites per person], most simulations within the space of parameter estimates for strain MM-CP (gray bars) resulted in the elimination of malaria transmission (Fig. 4B and fig. S7A). As transmission intensity increased (annual EIR, ~30), we detected a reduction in probability of elimination in the lower end of

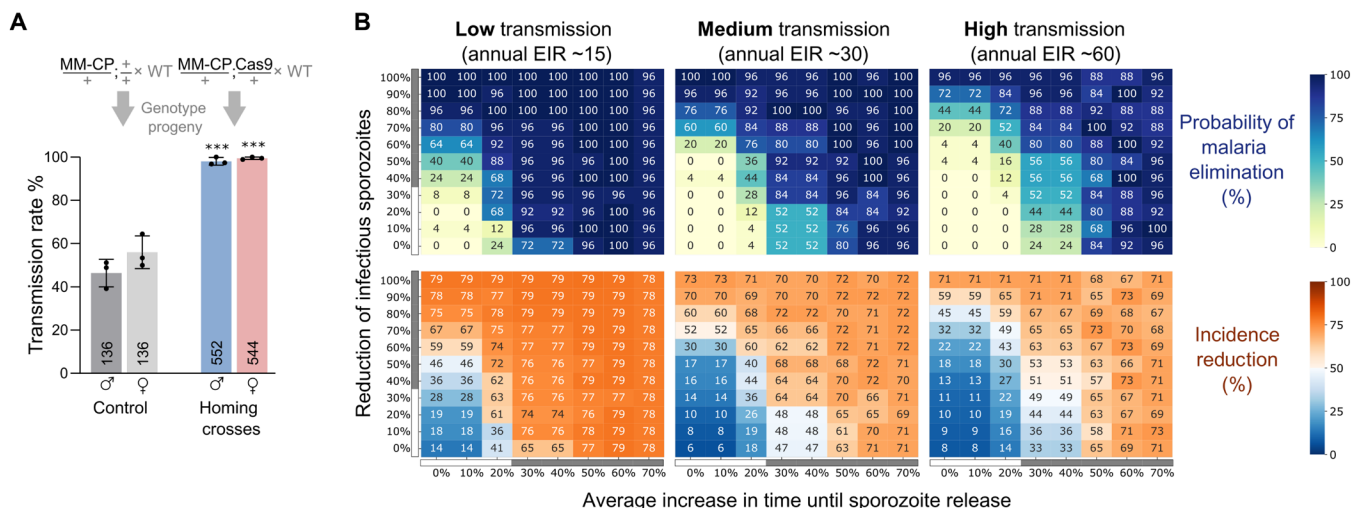


Fig. 4. Gene drive and predicted epidemiological impact of strain MM-CP deployment. (A) Assessment of nonautonomous gene drive in the progeny of male and female hemizygous MM-CP mosquitoes in the presence or absence of a vasa-Cas9 driver crossed to the WT. Larval offspring were subjected to multiplex PCR genotyping, and the mean and standard error (SEM) from three biological replicates is plotted, and the total number n is indicated. Statistical significance was determined using a one-way analysis of variance (ANOVA) with Tukey's correction. *** $P \leq 0.001$. (B) Heatmaps depicting elimination probabilities (top) and number of clinical cases reduced (bottom) at the end of 6 years following a single release of 1000 homozygous MM-CP mosquitoes that also carry a Cas9 IGD. Three transmission scenarios with varying EIRs for *P. falciparum* as a measure of exposure to infectious mosquitoes were explored. Homozygous transgenic mosquitoes are released 6 months after the start of the simulation in highly seasonal transmission settings of varying intensities. The parameter range that we explored for the reduction of the number of infectious sporozoites is represented on the major y axis, while the range for the average increase in time until sporozoites are released is represented on the major x axis. Parameter range estimates based on the experimental data for strain MM-CP are indicated next to the axes (gray bars).

the parameter estimate range (Fig. 4B and fig. S7B). In a high transmission scenario, a high reduction in sporozoite production in combination with a large delay was necessary for elimination to be triggered in the model (Fig. 4B and fig. S7C). However, note that significant reductions in clinical cases occurred even when elimination was not achieved. Therefore, in high transmission settings, even when not achieving elimination alone, MM-CP could open a window for elimination by strategically deploying other interventions that could act synergistically to drive transmission to zero.

DISCUSSION

CRISPR-Cas9 gene drives aimed at suppressing mosquito populations have seen much progress and publicity. Gene drives aimed at modifying mosquito populations, by directly interfering with their vectorial capacity, have not been in the spotlight to the same degree as they face an additional hurdle: the lack of a robust mechanism to interfere with *Plasmodium* development in genetically modified mosquitoes. This is despite research on such mechanisms predating the gene drive field by more than a decade. Any such mechanism must eventually hold up against the high genetic diversity of malaria parasites. The effector mechanism that we present here can bridge this gap. It is based on a minimal modification of an endogenous *A. gambiae* genomic locus to express two exogenous AMPs acting against malaria parasites in the mosquito midgut. We show that this modification impedes transmission of two different *Plasmodium* species, the deadliest human parasite *P. falciparum* and the rodent parasite *P. berghei*. It achieves this by hampering parasite sporogonic development that occurs in the oocyst, markedly delaying the emergence of infectious sporozoites, and we attribute this effect to the known propensity of these AMPs for interfering with mitochondrial function. As the modification additionally reduces female mosquito life span, the possibility of infectious sporozoites to be transmitted to a new host is reduced markedly.

Modeling suggests that propagation of this modification via gene drive promises to break the malaria transmission cycle across a range of epidemiological scenarios in sub-Saharan Africa even if the effector itself is eventually replaced by resistant alleles because of the fitness cost that it imposes. This modification is already designed for gene drive and requires no further adjustment before deployment, while, at the same time, it is inert on its own and thus can be safely tested in an endemic setting under standard containment protocols. It thus enables the next step for testing antimalarial effectors, i.e., to evaluate their transmission blocking modifications against parasites directly sampled from patients in malaria endemic countries.

MATERIALS AND METHODS

Design and generation of constructs

Annotated DNA sequence files for the final transformation constructs pD-Gam1-MM and pD-MM-CP are provided in file S1. Briefly, the 23 N-terminal amino acids of Cecropin 1 (Cec1, CecA, and AGAP000693) and Cecropin 2 (Cec2, CecB, and AGAP000692) served as secretion signals. Magainin 2, melittin, T2A, and P2A were codon usage optimized for *A. gambiae*, and the intron located within the melittin coding sequence was previously described (42) except for the SV40 terminator within the 3xP3-EGFP (enhanced GFP) marker module for which we swapped in the trypsin terminator (50). We first neutralized a Bsa I site in the ampicillin resistance

cassette and gene-synthesized (Genewiz) a fragment ranging from the Cecropin 1 secretion signal to the trypsin terminator, including 18-bp overlaps with the vector backbone and EGFP for subsequent Gibson Assembly. The marker-module and the U6 promoter were PCR-amplified from pI-Scorpine (42) with primers 78-GFP-R and 167-U6-R. The fragment from the Bsa I spacer to the P2A was synthesized (Genewiz), including 18-bp overlaps to the U6 promoter and the vector backbone. The vector backbone was PCR-amplified from pAmpR_SDM with primers 168-BBmut-F and 169-BBmut-R, and last, the four fragments were joined via Gibson Assembly to yield the intermediate plasmid pI-MM. The CP gRNA spacer (42) was inserted via the Bsa I sites, and the cassette was amplified with primers 172-CP-HA3-F-degen and 173-CP-HA5-R-Cec1 and fused with the CP homology arms and backbone amplified from pD-Sco-CP (42) with primers 170-Cec1-SS-F and 171-P2A-R to assemble the donor plasmid pD-MM-CP. A 5' P2A was added to the cassette via Golden Gate cloning of the annealed oligos 182-P2Aanneal-F and 183-P2Aanneal-R into Bgl II digested plasmid pI-MM, and subsequently, the Gam1 gRNA spacer (5'-TACAGAATGTTCTTCTGAG-3') was inserted via Bsa I. The gRNA sequence was chosen using Deskgen (Desktop Genetics, LTD) with an activity score of 54 and an off-target score of 99. The effector cassette was amplified with primers 184-P2Adegen-F and 185-Mel-R and fused via Gibson Assembly with the gambicin homology arms amplified from G3 genomic DNA (gDNA) and the backbone to generate the donor plasmid pD-Gam1-MM. For primers, see table S2.

Transgenesis and establishment of markerless strains

A. gambiae G3 eggs were injected with the corresponding donor plasmids pD-MM-CP or pD-Gam1-MM and the Cas9 helper plasmid p155 (4). Twenty-five F1 transgenics were obtained for MM^{GFP}-CP and one female F1 transgenic for Gam1-MM^{GFP}. MM^{GFP}-CP was established from a founder cage with nine females, and F1 individuals were confirmed by Sanger sequencing with primers EGFP-C-For, 117-CP-ctrl-R, and 163-P3-probe-F and Gam1-MM^{GFP} with primers EGFP-C-For and EGFP-N. Transgenics were outcrossed to G3 WT over three generations for Gam1-MM^{GFP} and two generations for MM^{GFP}-CP before crossing to the vasa-Cre (51) strain in the KIL background. Larval offspring were screened for GFP and DsRed, and siblings were mated. The progeny was screened against GFP and DsRed; pupae were singled out, and the exuviate was collected for genotyping with primers 99-CP-locus-F and 100-CP-locus-R or 241-Gam-locus-F and 242-Gam-locus-R, respectively, to identify homozygotes. The markerless line MM-CP was established from 9 males and 11 females. For Gam1-MM, three cups with one female and one male and six cups with two males and two females were set up and pooled after confirmation via Sanger sequencing. A G3-KIL mixed colony was used as WT control for all experiments, unless otherwise stated. All experiments were performed with cow blood [First Link (UK) Ltd.], unless otherwise stated.

RT-PCR and splicing analysis

MM-CP and the WT control were fed with human blood, and midguts were dissected after 3 hours. For Gam1-MM, this experiment was performed on unfed females. Thirty guts were lysed in TRIzol and homogenized with 2.8-mm ceramic beads (CK28R, Precellys) for 30 s at 6800 rpm in a Precellys 24 homogenizer (Bertin). RNA was extracted with the Direct-zol RNA Mini-prep kit (Zymo Research) including on-column deoxyribonuclease (DNase) treatment and

transcribed into cDNA with the qScript cDNA Synthesis Kit (Quantabio). RT-PCR was performed with a Phire Tissue Direct PCR Master Mix kit (Thermo Scientific) using primers 429-Gambicin-F and 430-Gambicin-R, 270-qCP-F1 and 271-qCP-R3, 484-qMag-both-F and 485-qMel-both-R, and 447-S7-F and 448-S7-R for the S7 reference gene. To quantify splicing efficiency, PCRs were performed on above cDNAs with Q5 High-Fidelity DNA Polymerase (NEB) using 484-qMag-both-F as forward primer and 242-Gam-locus-R (365-bp amplicon) or 246-qCP-R2 (309 bp) as reverse primer, respectively. Annealing temperature, extension time, and cycle number were set to 67°C, 5 s, and 27 cycles, respectively. Amplicons were purified with the QIAquick PCR Purification Kit (QIAGEN) and submitted to Amplicon-EZ NGS (Genewiz), and the data (GenBank accession PRJNA778891) were analyzed using Geneious Prime (Biomatters).

Mosquito infection assays

Transgenic or control mosquitoes were infected with mature *P. falciparum* NF54 gametocyte cultures (2 to 6% gametocytemia) as described previously using the streamlined standard membrane feeding assay (29) or with *P. berghei* ANKA 2.34 that constitutively expresses GFP by direct feeding on infected mice. Engorged mosquitoes were provided 10% sucrose and maintained at 27°C for *P. falciparum* infections and 21°C/75% relative humidity for *P. berghei* infections until dissections were performed. Supplemental blood meals on human blood were provided via membrane feeding. For infections of mosquitoes with mature *P. falciparum*, mosquitoes were starved without sugar for 48 hours after the infective or supplemental blood meal to eliminate unfed individuals.

Analysis of parasite infection intensity and prevalence

We dissected midguts at the indicated days and microscopically examined them for the presence of oocysts after staining with 0.1% mercurochrome. We measured the diameter of oocyst using ImageJ (52). For measuring the prevalence and intensity of sporozoites, the head, thorax, and the midgut were dissected for each female. The gDNA was extracted separately from head/thorax samples and the corresponding midgut samples with the DNeasy 96 Blood and Tissue Kit (QIAGEN) and was used for qPCR 20- μ l reactions using a QIAGEN QuantiNova SYBR Green PCR kit to quantify the *P. falciparum* Cyt-B gene fragment using primers and methods described previously (43, 53). Standard curves for the target gene and the *A. gambiae* S7 reference gene were calculated after serial dilution of nucleic acid templates. C_t values were converted using their respective standard curves, and the target gene C_t value was normalized to the reference gene (*A. gambiae* S7 ribosomal gene).

Generation of backcross populations and genotyping

Fifty homozygous MM-CP males and females were crossed to 50 *A. gambiae* s.s. Ifakara strain females and males, respectively. F1 siblings were mass-mated in a single cage to obtain F2 progeny. F2 females were used for infection experiments or survival assays as described. For genotyping of individual mosquitoes, we used multiplex genomic PCR with primers CP-multi-F, CP-multi-R, and Mag-R, which results in a 356-bp amplicon for the MM-CP transgene and 670 bp for the unmodified CP locus.

Fitness and survival assays

For each replicate, 20 females were individually transferred to cups 1 day after being offered an uninfected blood meal. Spermathecae

were dissected from females that failed to produce eggs or larvae and thus determine whether they were fertilized by sperm. Unfertilized females were excluded from the analysis. Eggs and larvae were counted on day 7 after blood feed. To determine the pupal sex ratio and pupation time, 100 L1 larvae per tray were reared to the pupal stage where pupae were being collected and sexed once a day. Three biological replicates were performed, and the data were analyzed via the chi-square test for deviations from the expected sex ratio of 50%. The average pupation time in days was calculated and tested for statistical significance with the Mann-Whitney test. For the survival analysis including both sexes, a total of 274 WT and 276 MM-CP male and 275 WT and 304 MM-CP female pupae were placed in six separate cages with bottles containing 10% filtered fructose solution, and accumulated dead mosquitoes were counted daily. Survival was monitored daily for 44 days on three independent replicates. For the survival analysis of backcrossed females, F2 mosquitoes were placed in W24.5 cm by D24.5 cm by H24.5 cm cages as pupae. Mosquitoes were offered a 10% sugar solution, and they were also offered a blood meal and allowed to deposit eggs 72 hours after every blood meal. Dead mosquitoes were collected every 24 hours from the cage and preserved to be genotyped. Survival was monitored daily for 25 days on two independent replicates.

RNA-seq analysis

Females were fed with human blood, and 15 guts were dissected into TRIzol after 6 hours, after 20 hours, and from unfed females. After homogenization with 2.8-mm ceramic beads (CK28R, Precellys), RNA was extracted with the Direct-zol RNA Mini-prep Kit (Zymo Research) including on-column DNase treatment. Four biological replicates per condition were subjected to RNA sequencing (RNA-seq). Libraries were prepared with the NEB Next Ultra RNA Library Prep Kit and sequenced on a NovaSeq 6000 Illumina platform (instrument HWI-ST1276) generating 150-bp paired-end reads (GenBank accession PRJNA822650). Replicate 1 for MM-CP without blood meal (MMCP_N_1) was identified as outlier with squared Pearson correlation coefficients with the other three biological replicates below 0.84 and hence removed from further analysis. Sequencing reads were mapped to the *A. gambiae* PEST genome (AgamP4.13, GCA_000005575.2 supplemented with the MM-CP construct reference) using HISAT2 software v2.0.5 (with parameters --dta --phred33) (54). Differential expression was assessed with DESeq2 v1.20.0. GO enrichment analysis was performed using TopGO (55) with a pruning factor of 50 using a *P* value cutoff of *P* = 0.01.

Assessment of nonautonomous gene drive

At least 60 homozygous MM-CP or WT females were crossed to males of the vasa-Cas9 strain. F1 progeny were screened for the presence of the 3xP3-YFP marker, and transhemizygotes were then sexed and crossed to WT. gDNA was isolated from the progeny at the L2-L3 larval stage according to the protocol of the Phire Tissue Direct PCR Kit (Thermo Scientific). Multiplex PCR was performed with primers 260-q-Mag-Mel-R, 531-CP-multi-R, and 532-CP-multi-F, yielding a 356-bp band if the construct is present and a WT band of 670 bp as control. Two 96-well-plates per parent (paternal or maternal transhemizygotes) and replicate were analyzed, and four negative controls were included on each plate. From the control crosses, 46 offspring per parent were analyzed for each replicate. The homing rate was calculated as $(n \times 0.5 - E_{\text{neg}})/(n \times 0.5) \times 100$, with E_{neg}

being the individuals negative for the effector and n being the total number of samples successfully analyzed by PCR.

Transmission modeling using EMOD

Simulations were performed using EMOD v2.20 (56), a mechanistic, agent-based model of *P. falciparum* malaria transmission that include vector life cycle dynamics and within host-parasite and immune dynamics. Seasonality of rainfall and temperature as well as vector species were kept the same across transmission settings, but vector density was varied to match desired transmission intensity. *A. gambiae*, the only vector considered, was assumed as being 95% endophilic and 65% anthropophilic. Each simulation contained 1000 representative people with birth and death rates appropriate to the demography without considering importation of malaria. We include baseline health seeking for symptomatic cases as an intervention where human agents can seek treatment with 80% artemether-lumefantrine of the time within 2 days of severe symptom onset and 50% of the time within 3 days of the onset of a clinical but nonsevere case. Mosquitoes within EMOD contain simulated genomes that can model up to 10 genes with eight alleles per gene with phenotypic traits that map onto different genotypes (49). Here, we modeled an IGD system (57) aimed at population replacement with an effector that results in delayed sporozoite production in infected mosquitoes and overall reduction in the number of sporozoites produced by infected mosquitoes. The model was further parameterized using the experimentally determined measures of fitness, life span, and homing. One thousand male IGD mosquitoes homozygous for the autonomous drive (Cas9) and nonautonomous effector (MM-CP) were released just before the wet season begins to pick up in transmission intensity (table S2). Apart from the sex chromosomes, two loci representing the effector and driver were modeled (57), with each locus having four possible alleles (WT, resistant, effector, or nuclease and loss of gene function for the effector or driver locus). To evaluate the performance of these drives in a range of transmission settings, we vary transmission intensity via annual entomological rates (EIR) ranging from 15 infectious bites per person to 60 infectious bites per person. We also vary the final phenotypic effect of expressing the effector gene that leads to delayed and reduced sporozoite formation. We evaluate average increases in time until sporozoite formation ranging from no increase in time compared to a WT mosquito up to 70% increase in sporozoite formation time. As for the reduced sporozoite effect, we evaluated to full range of possible effects compared to a WT mosquito. Mosquitoes carrying the drive are released 6 months into the simulation, and simulations are run for a total of 6 years. The outputs represent the mean of 25 stochastic realizations per parameter set.

SUPPLEMENTARY MATERIALS

Supplementary material for this article is available at <https://science.org/doi/10.1126/sciadv.abo1733>

REFERENCES AND NOTES

- World Health Organization, *World Malaria Report 2020: 20 Years of Global Progress and Challenges* (World Health Organization, 2020).
- M. B. Laurens, RTS,S/AS01 vaccine (Mosquirix): An overview. *Hum. Vaccin. Immunother.* **16**, 480–489 (2020).
- N. Windbichler, M. Menichelli, P. A. Papathanos, S. B. Thyme, H. Li, U. Y. Ulge, B. T. Hovde, D. Baker, R. J. Monnat, A. Burt, A. Crisanti, A synthetic homing endonuclease-based gene drive system in the human malaria mosquito. *Nature* **473**, 212–215 (2011).
- A. Hammond, R. Galizi, K. Kyrou, A. Simoni, C. Siniscalchi, D. Katsanos, M. Gribble, D. Baker, E. Marois, S. Russell, A. Burt, N. Windbichler, A. Crisanti, T. Nolan, A CRISPR-Cas9 gene drive system targeting female reproduction in the malaria mosquito vector *Anopheles gambiae*. *Nat. Biotechnol.* **34**, 78–83 (2016).
- K. Kyrou, A. M. Hammond, R. Galizi, N. Kranjc, A. Burt, A. K. Beaghton, T. Nolan, A. Crisanti, A CRISPR-Cas9 gene drive targeting doublesex causes complete population suppression in caged *Anopheles gambiae* mosquitoes. *Nat. Biotechnol.* **36**, 1062–1066 (2018).
- A. Hammond, X. Karlsson, I. Morianou, K. Kyrou, A. Beaghton, M. Gribble, N. Kranjc, R. Galizi, A. Burt, A. Crisanti, T. Nolan, Regulating the expression of gene drives is key to increasing their invasive potential and the mitigation of resistance. *PLOS Genet.* **17**, e1009321 (2021).
- V. M. Gantz, N. Jasinskiene, O. Tatarenkova, A. Fazekas, V. M. Macias, E. Bier, A. A. James, Highly efficient Cas9-mediated gene drive for population modification of the malaria vector mosquito *Anopheles stephensi*. *Proc. Natl. Acad. Sci. U.S.A.* **112**, E6736–E6743 (2015).
- T. B. Pham, C. H. Phong, J. B. Bennett, K. Hwang, N. Jasinskiene, K. Parker, D. Stillinger, J. M. Marshall, R. Carballar-Lejarazu, A. A. James, Experimental population modification of the malaria vector mosquito, *Anopheles stephensi*. *PLOS Genet.* **15**, e1008440 (2019).
- A. Adolphi, V. M. Gantz, N. Jasinskiene, H. F. Lee, K. Hwang, G. Terradas, E. A. Bulger, A. Ramaiah, J. B. Bennett, J. J. Emerson, J. M. Marshall, E. Bier, A. A. James, Efficient population modification gene-drive rescue system in the malaria mosquito *Anopheles stephensi*. *Nat. Commun.* **11**, 5553 (2020).
- J. Ito, A. Ghosh, L. A. Moreira, E. A. Wimmer, M. Jacobs-Lorena, Transgenic anopheline mosquitoes impaired in transmission of a malaria parasite. *Nature* **417**, 452–455 (2002).
- L. A. Moreira, J. Ito, A. Ghosh, M. Devenport, H. Zieher, E. G. Abraham, A. Crisanti, T. Nolan, F. Catteruccia, M. Jacobs-Lorena, Bee venom phospholipase inhibits malaria parasite development in transgenic mosquitoes. *J. Biol. Chem.* **277**, 40839–40843 (2002).
- W. Kim, H. Koo, A. M. Richman, D. Seeley, J. Vizioli, A. D. Klocko, D. A. O'brotcha, Ectopic expression of a cecropin transgene in the human malaria vector mosquito *Anopheles gambiae* (Diptera: Culicidae): Effects on susceptibility to *Plasmodium*. *J. Med. Entomol.* **41**, 447–455 (2004).
- E. G. Abraham, M. Donnelly-Doman, H. Fujioka, A. Ghosh, L. Moreira, M. Jacobs-Lorena, Driving midgut-specific expression and secretion of a foreign protein in transgenic mosquitoes with AgAper1 regulatory elements. *Insect Mol. Biol.* **14**, 271–279 (2005).
- V. Corby-Harris, A. Drexler, L. Watkins de Jong, Y. Antonova, N. Pakpour, R. Ziegler, F. Ramberg, E. E. Lewis, J. M. Brown, S. Luckhart, M. A. Riehle, Activation of Akt signaling reduces the prevalence and intensity of malaria parasite infection and lifespan in *Anopheles stephensi* mosquitoes. *PLOS Pathog.* **6**, e1001003 (2010).
- J. M. Meredith, S. Basu, D. D. Nimmo, I. Larget-Thiery, E. L. Warr, A. Underhill, C. C. McArthur, V. Carter, H. Hurd, C. Bourgoin, P. Eggleston, Site-specific integration and expression of an anti-malarial gene in transgenic *Anopheles gambiae* significantly reduces *Plasmodium* infections. *PLOS One* **6**, e14587 (2011).
- A. T. Isaacs, F. Li, N. Jasinskiene, X. Chen, X. Nirmala, O. Marinotti, J. M. Vinetz, A. A. James, Engineered resistance to *Plasmodium falciparum* development in transgenic *Anopheles stephensi*. *PLOS Pathog.* **7**, e1002017 (2011).
- A. T. Isaacs, N. Jasinskiene, M. Tretiakov, I. Thiery, A. Zettor, C. Bourgoin, A. A. James, Transgenic *Anopheles stephensi* coexpressing single-chain antibodies resist *Plasmodium falciparum* development. *Proc. Natl. Acad. Sci. U.S.A.* **109**, E1922–E1930 (2012).
- E. S. Hauck, Y. Antonova-Koch, A. Drexler, J. Pietri, N. Pakpour, D. Liu, J. Blacutt, M. A. Riehle, S. Luckhart, Overexpression of phosphatase and tensin homolog improves fitness and decreases *Plasmodium falciparum* development in *Anopheles stephensi*. *Microbes Infect.* **15**, 775–787 (2013).
- A. J. Arik, L. V. Hun, K. Quicke, M. Piatt, R. Ziegler, P. Y. Scaraffia, H. Badgandi, M. A. Riehle, Increased Akt signaling in the mosquito fat body increases adult survivorship. *FASEB J.* **29**, 1404–1413 (2015).
- G. Volohonsky, A. K. Hopp, M. Saenger, J. Soichot, H. Scholze, J. Boch, S. A. Blandin, E. Marois, Transgenic expression of the anti-parasitic factor TEP1 in the malaria mosquito *Anopheles gambiae*. *PLOS Pathog.* **13**, e1006113 (2017).
- M. L. Simões, Y. Dong, A. Hammond, A. Hall, A. Crisanti, T. Nolan, G. Dimopoulos, The *Anopheles* FBN9 immune factor mediates *Plasmodium* species-specific defense through transgenic fat body expression. *Dev. Comp. Immunol.* **67**, 257–265 (2017).
- S. Dong, X. Fu, Y. Dong, M. L. Simões, J. Zhu, G. Dimopoulos, Broad spectrum immunomodulatory effects of *Anopheles gambiae* microRNAs and their use for transgenic suppression of *Plasmodium*. *PLOS Pathog.* **16**, e1008453 (2020).
- Y. Dong, M. L. Simoes, G. Dimopoulos, Versatile transgenic multistage effector-gene combinations for *Plasmodium falciparum* suppression in *Anopheles*. *Sci. Adv.* **6**, eaay5898 (2020).
- V. Carter, H. Hurd, Choosing anti-*Plasmodium* molecules for genetically modifying mosquitoes: Focus on peptides. *Trends Parasitol.* **26**, 582–590 (2010).
- A. Bell, Antimalarial peptides: The long and the short of it. *Curr. Pharm. Des.* **17**, 2719–2731 (2011).
- S. Wang, M. Jacobs-Lorena, Genetic approaches to interfere with malaria transmission by vector mosquitoes. *Trends Biotechnol.* **31**, 185–193 (2013).

27. N. Vale, L. Aguiar, P. Gomes, Antimicrobial peptides: A new class of antimalarial drugs? *Front. Pharmacol.* **5**, 275 (2014).
28. V. Carter, A. Underhill, I. Baber, L. Sylla, M. Baby, I. Larget-Thierry, A. Zettor, C. Bourgoign, Ü. Langel, I. Faye, L. Otvos, J. D. Wade, M. B. Coulibaly, S. F. Traore, F. Tripet, P. Eggleston, H. Hurd, Killer bee molecules: Antimicrobial peptides as effector molecules to target sporogonic stages of *Plasmodium*. *PLOS Pathog.* **9**, e1003790 (2013).
29. T. Habtewold, S. Tapanelli, E. K. G. Masters, A. Hoermann, N. Windbichler, G. K. Christophides, Streamlined SMFA and mosquito dark-feeding regime significantly improve malaria transmission-blocking assay robustness and sensitivity. *Malar. J.* **18**, 24 (2019).
30. E. Martin, T. Ganz, R. I. Lehrer, Defensins and other endogenous peptide antibiotics of vertebrates. *J. Leukoc. Biol.* **58**, 128–136 (1995).
31. A. Giuliani, G. Pirri, S. F. Nicoletto, Antimicrobial peptides: An overview of a promising class of therapeutics. *Cent. Eur. J. Biol.* **2**, 1–33 (2007).
32. Z. Ahmad, T. F. Laughlin, Medicinal chemistry of ATP synthase: A potential drug target of dietary polyphenols and amphibian antimicrobial peptides. *Curr. Med. Chem.* **17**, 2822–2836 (2010).
33. H. Moravej, Z. Moravej, M. Yazdanparast, M. Heiat, A. Mirhosseini, M. Moosazadeh Moghaddam, R. Mirnejad, Antimicrobial peptides: Features, action, and their resistance mechanisms in bacteria. *Microb. Drug Resist.* **24**, 747–767 (2018).
34. D. Zhang, Y. He, Y. Ye, Y. Ma, P. Zhang, H. Zhu, N. Xu, S. Liang, Little antimicrobial peptides with big therapeutic roles. *Protein Pept. Lett.* **26**, 564–578 (2019).
35. K. Matsuzaki, O. Murase, N. Fujii, K. Miyajima, An antimicrobial peptide, magainin 2, induced rapid flip-flop of phospholipids coupled with pore formation and peptide translocation. *Biochemistry* **35**, 11361–11368 (1996).
36. L. Yang, T. A. Harroun, T. M. Weiss, L. Ding, H. W. Huang, Barrel-stave model or toroidal model? A case study on melittin pores. *Biophys. J.* **81**, 1475–1485 (2001).
37. M. Hugosson, D. Andreu, H. G. Boman, E. Glaser, Antibacterial peptides and mitochondrial presequences affect mitochondrial coupling, respiration and protein import. *Eur. J. Biochem.* **223**, 1027–1033 (1994).
38. J. R. Gledhill, J. E. Walker, Inhibition sites in F1-ATPase from bovine heart mitochondria. *Biochem. J.* **386**, 591–598 (2005).
39. T. F. Laughlin, Z. Ahmad, Inhibition of *Escherichia coli* ATP synthase by amphibian antimicrobial peptides. *Int. J. Biol. Macromol.* **46**, 367–374 (2010).
40. H. V. Westerhoff, D. Juretic, R. W. Hendler, M. Zasloff, Magainins and the disruption of membrane-linked free-energy transduction. *Proc. Natl. Acad. Sci. U.S.A.* **86**, 6597–6601 (1989).
41. R. W. Gwadz, D. Kaslow, J. Y. Lee, W. L. Maloy, M. Zasloff, L. H. Miller, Effects of magainins and cecropins on the sporogonic development of malaria parasites in mosquitoes. *Infect. Immun.* **57**, 2628–2633 (1989).
42. A. Hoermann, S. Tapanelli, P. Capriotti, G. del Corzano, E. K. G. Masters, T. Habtewold, G. K. Christophides, N. Windbichler, Converting endogenous genes of the malaria mosquito into simple non-autonomous gene drives for population replacement. *eLife* **10**, e58791 (2021).
43. T. Habtewold, A. A. Sharma, C. A. S. Wyer, E. K. G. Masters, N. Windbichler, G. K. Christophides, *Plasmodium* oocysts respond with dormancy to crowding and nutritional stress. *Sci. Rep.* **11**, 3090 (2021).
44. W. R. Shaw, I. E. Holmdahl, M. A. Itoe, K. Werling, M. Marquette, D. G. Paton, N. Singh, C. O. Buckee, L. M. Childs, F. Catteruccia, Multiple blood feeding in mosquitoes shortens the *Plasmodium falciparum* incubation period and increases malaria transmission potential. *PLOS Pathog.* **16**, e1009131 (2020).
45. H. Ke, I. A. Lewis, J. M. Morrissey, K. J. McLean, S. M. Ganesan, H. J. Painter, M. W. Mather, M. Jacobs-Lorena, M. Llinás, A. B. Vaidya, Genetic investigation of tricarboxylic acid metabolism during the *Plasmodium falciparum* life cycle. *Cell Rep.* **11**, 164–174 (2015).
46. C. D. Goodman, J. E. Siregar, V. Mollard, J. Vega-Rodríguez, D. Syafruddin, H. Matsuoka, M. Matsuzaki, T. Toyama, A. Sturm, A. Cozijnsen, M. Jacobs-Lorena, K. Kita, S. Marzuki, G. I. McFadden, Parasites resistant to the antimalarial atovaquone fail to transmit by mosquitoes. *Science* **352**, 349–353 (2016).
47. A. Sturm, V. Mollard, A. Cozijnsen, C. D. Goodman, G. I. McFadden, Mitochondrial ATP synthase is dispensable in blood-stage *Plasmodium berghei* rodent malaria but essential in the mosquito phase. *Proc. Natl. Acad. Sci. U.S.A.* **112**, 10216–10223 (2015).
48. J. M. Matz, C. Goosmann, K. Matuschewski, T. W. A. Kooij, An unusual prohibitin regulates malaria parasite mitochondrial membrane potential. *Cell Rep.* **23**, 756–767 (2018).
49. P. Selvaraj, E. A. Wenger, D. Bridenbecker, N. Windbichler, J. R. Russell, J. Gerardin, C. A. Bever, M. Nikolov, Vector genetics, insecticide resistance and gene drives: An agent-based modeling approach to evaluate malaria transmission and elimination. *PLoS Comput. Biol.* **16**, e1008121 (2020).
50. S. Yoshida, Y. Shimada, D. Kondoh, Y. Kouzuma, A. K. Ghosh, M. Jacobs-Lorena, R. E. Sinden, Hemolytic C-type lectin CEL-III from sea cucumber expressed in transgenic mosquitoes impairs malaria parasite development. *PLOS Pathog.* **3**, e192 (2007).
51. G. Volohonsky, O. Terenzi, J. Soichot, D. A. Naujoks, T. Nolan, N. Windbichler, D. Kapps, A. L. Smidler, A. Vittu, G. Costa, S. Steinert, E. A. Levashina, S. A. Blandin, E. Marois, Tools for *Anopheles gambiae* transgenesis. *G3* **5**, 1151–1163 (2015).
52. W. S. Rasband, ImageJ. U. S. National Institutes of Health, <https://imagej.nih.gov/ij/> (1997–2018).
53. C. Farrugia, O. Cabaret, F. Botterel, C. Bories, F. Foulet, J. M. Costa, S. Bretagne, Cytochrome b gene quantitative PCR for diagnosing *Plasmodium falciparum* infection in travelers. *J. Clin. Microbiol.* **49**, 2191–2195 (2011).
54. D. Kim, J. M. Paggi, C. Park, C. Bennett, S. L. Salzberg, Graph-based genome alignment and genotyping with HISAT2 and HISAT-genotype. *Nat. Biotechnol.* **37**, 907–915 (2019).
55. J. R. Adrian Alexa, topGO: Enrichment Analysis for Gene Ontology. R package version 2.38.1., (2019).
56. A. Bershteyn, J. Gerardin, D. Bridenbecker, C. W. Lorton, J. Bloedow, R. S. Baker, G. Chabot-Couture, Y. Chen, T. Fischle, K. Frey, J. S. Gauld, H. Hu, A. S. Izzo, D. J. Klein, D. Lukacevic, K. A. McCarthy, J. C. Miller, A. L. Ouedraogo, T. A. Perkins, J. Steinkraus, Q. A. ten Bosch, H. F. Ting, S. Titova, B. G. Wagner, P. A. Welkhoff, E. A. Wenger, C. N. Wiswell; Institute for Disease Modeling, Implementation and applications of EMOD, an individual-based multi-disease modeling platform. *Pathog. Dis.* **76**, fty059 (2018).
57. A. Nash, G. M. Urdaneta, A. K. Beaghton, A. Hoermann, P. A. Papanthanos, G. K. Christophides, N. Windbichler, Integral gene drives for population replacement. *Biol. Open* **8**, bio037762 (2019).

Acknowledgments: We thank E. Marois for sharing the vasa-Cre and vasa-Cas9 lines. We thank D. Bridenbecker for software support and A. Burt for suggestions on the manuscript. **Funding:** The work was funded by the Bill and Melinda Gates Foundation grant OPP1158151 to N.W. and G.K.C. and Wellcome Trust Investigator Award 107983/Z/15/Z to G.K.C. **Author contributions:** Conceptualization, data curation, formal analysis, investigation, methodology, visualization, and writing (preparation of original draft): A.H. and T.H. Investigation, methodology, software, visualization, and writing (preparation of original draft): P.S. Investigation and resources: G.D.C., P.C., M.G.I., and T.M.K. Conceptualization, funding acquisition, project management, supervision, and writing (review and editing): G.K.C. Conceptualization, funding acquisition, project management, supervision, writing (review and editing), formal analysis, and visualization: N.W. **Competing interests:** The authors declare that they have no competing interests. **Data and materials availability:** All data needed to evaluate the conclusions in the paper are present in the paper and/or the Supplementary Materials. Input data and scripts to generate the figure panels presented in the paper are available at Dryad (doi:10.5061/dryad.rfj6q57dq) or https://github.com/genome-traffic/anopheles_MM-CP_paper. As an additional resource, the EMOD gene drive model has been made available at https://github.com/InstituteForDiseaseModeling/sporogonic_retardation_2022. The RNA-seq raw data have been deposited to the National Center for Biotechnology Information NRA (PRJNA822650).

Submitted 18 January 2022
Accepted 4 August 2022
Published 21 September 2022
10.1126/sciadv.abo1733

Supplementary Materials for
Gene drive mosquitoes can aid malaria elimination by retarding *Plasmodium* sporogonic development

Astrid Hoermann *et al.*

Corresponding author: George K. Christophides, g.christophides@imperial.ac.uk;
Nikolai Windbichler, n.windbichler@imperial.ac.uk

Sci. Adv. **8**, eabo1733 (2022)
DOI: 10.1126/sciadv.abo1733

The PDF file includes:

Figs. S1 to S7
Tables S1 and S2
Legends for supplementary files S1 and S2

Other Supplementary Material for this manuscript includes the following:

Supplementary files S1 and S2

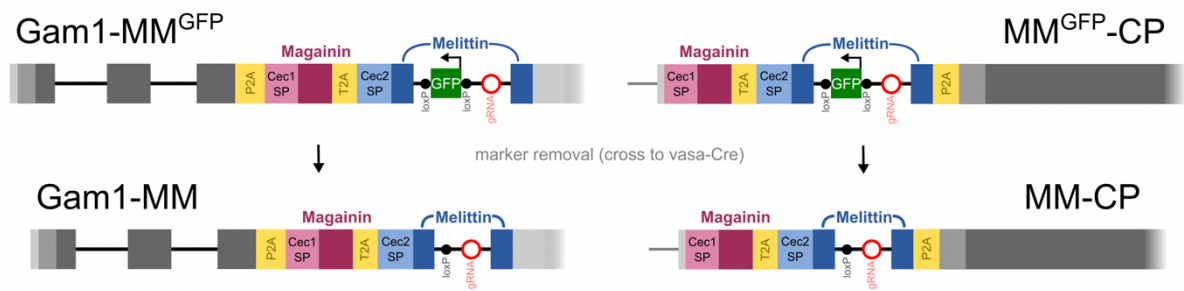


Fig. S1.

Schematic showing the inserted transgene constructs at the Gam1 or CP loci and the predicted exon structures following the excision of the GFP marker gene by Cre recombinase. The eGFP marker driven by the 3xP3 promoter and trypsin 3' UTR is shown in a simplified way and not to scale.

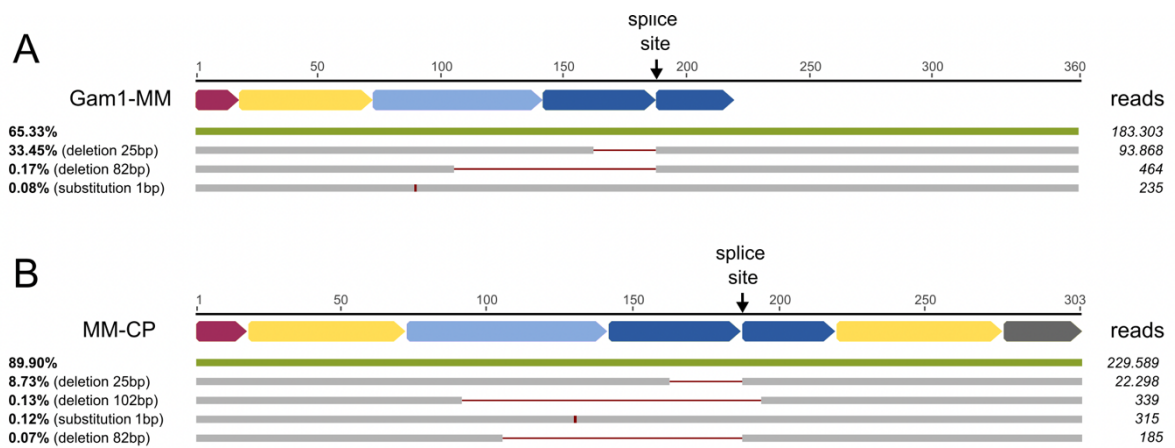


Fig. S2.

Alignment of sequenced cDNA amplicons to reference sequences representing the expected splicing outcomes for Gam1-MM and MM-CP. The splice site is indicated by the black arrow, the relative distribution of predicted variants (grey) representing at least 0.07% of all reads is shown on the left and the corresponding number of reads on the right.

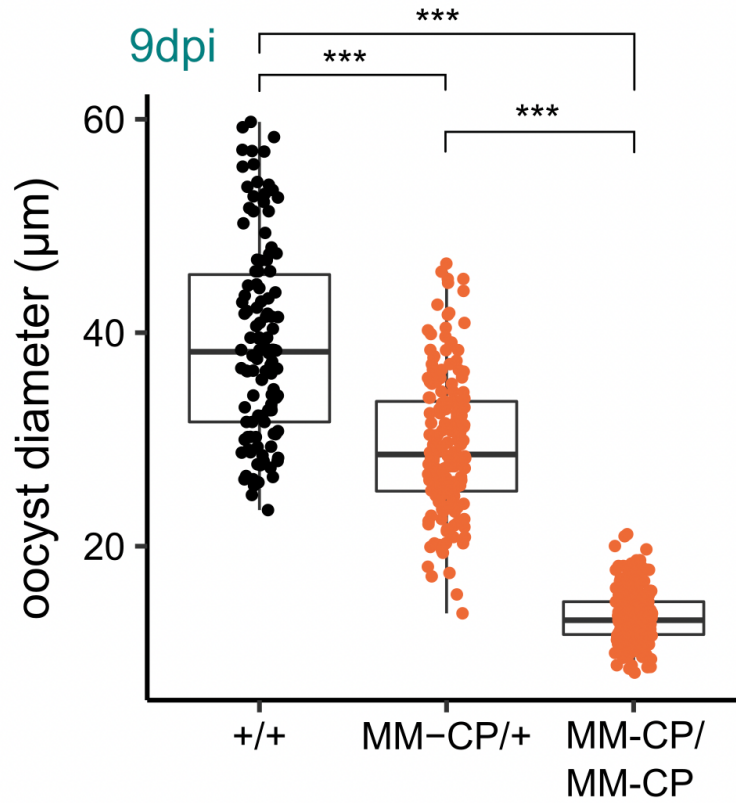


Fig. S3.

Quantification of *P. falciparum* oocyst diameter in F2 individuals following a backcross of strain MM-CP to the Ifakara strain and an F1 sibling intercross from 3 pooled biological replicates. Non-transgenic (+/+), hemizygous (MM-CP/+) and homozygous (MM-CP/MM-CP) individuals were identified by individual PCR genotyping after oocyst size had been determined. Statistical analysis was performed by a t-test assuming unequal variance.

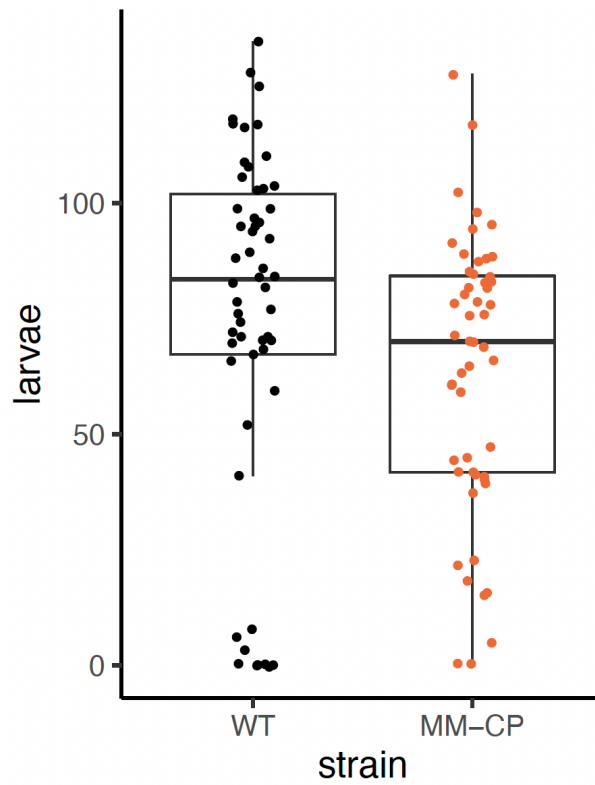


Fig. S4.

Larval output of individual homozygous MM-CP females compared to the wildtype (WT) obtained during the first gonotrophic cycle shows a 15.6% reduction ($p=0.079$). Data from 3 pooled biological replicates are shown. Statistical significance was determined by a t-test assuming unequal variance.

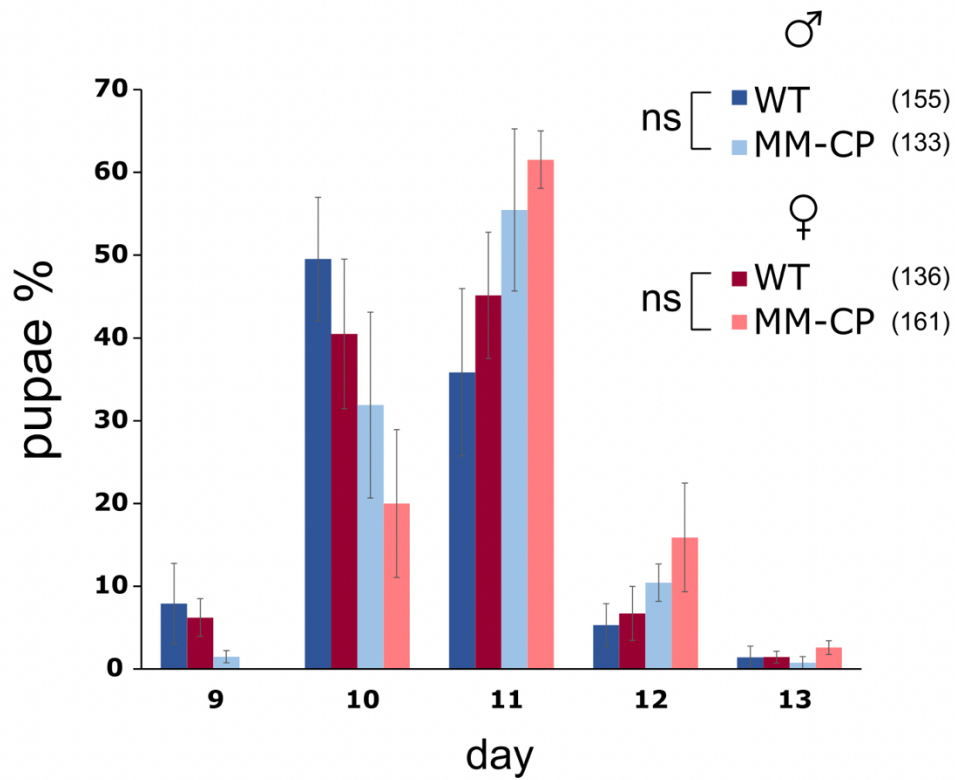


Fig. S5.

Analysis of the time of pupation of MM-CP and wild-type mosquitoes as the percentage of pupae emerging each day. Statistical analysis of average pupation times in males and females was calculated using the Mann-Whitney test.

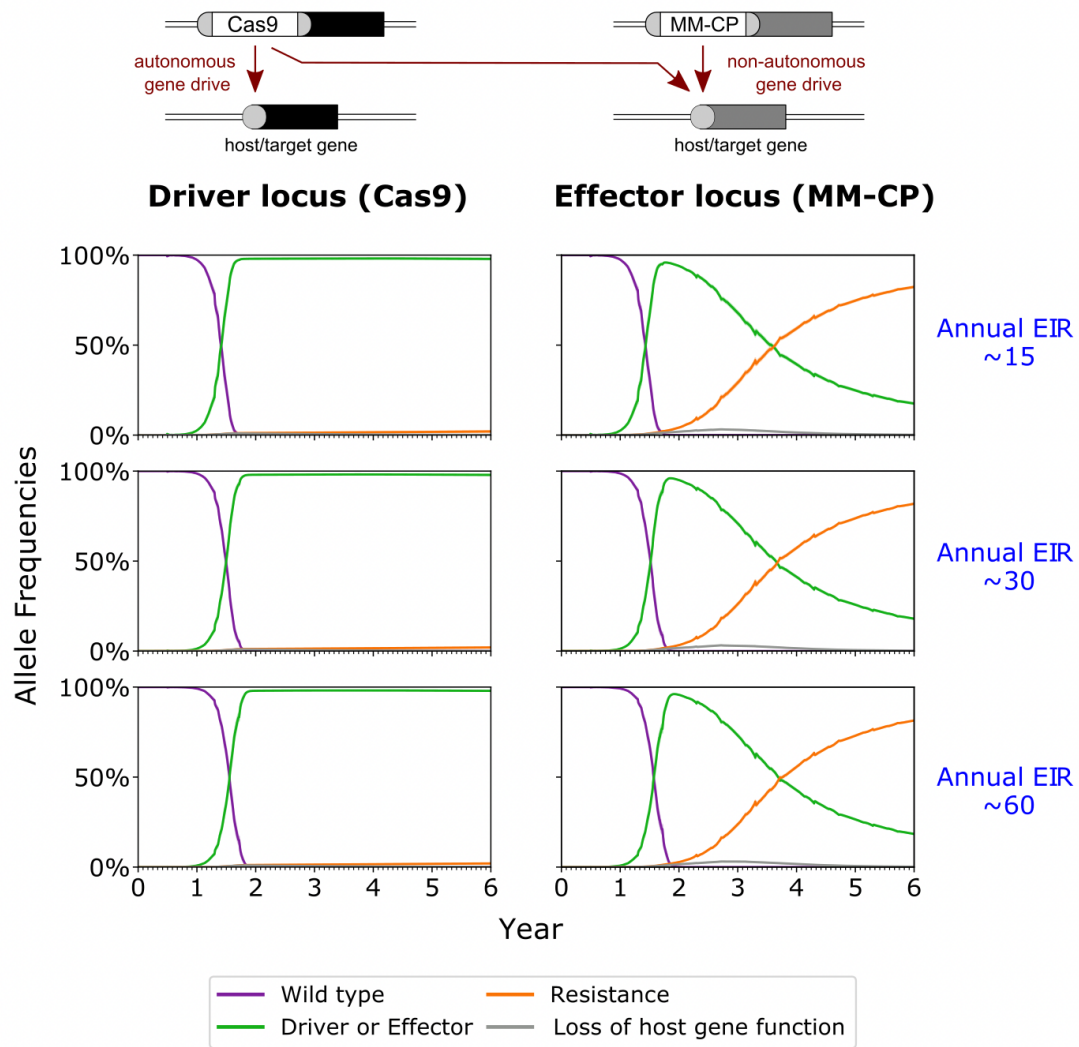


Fig. S6.

The mean time course of allele frequencies after 1000 gene drives mosquitoes homozygous for the driver and effector locus are released 6 months into a 6-year simulation. Each row represents a different transmission intensity. The left column depicts allele frequency at the driver locus and the right column represents allele frequencies at the effector locus. Shown is the mean allele frequency as calculated from 25 stochastic realizations of each scenario.

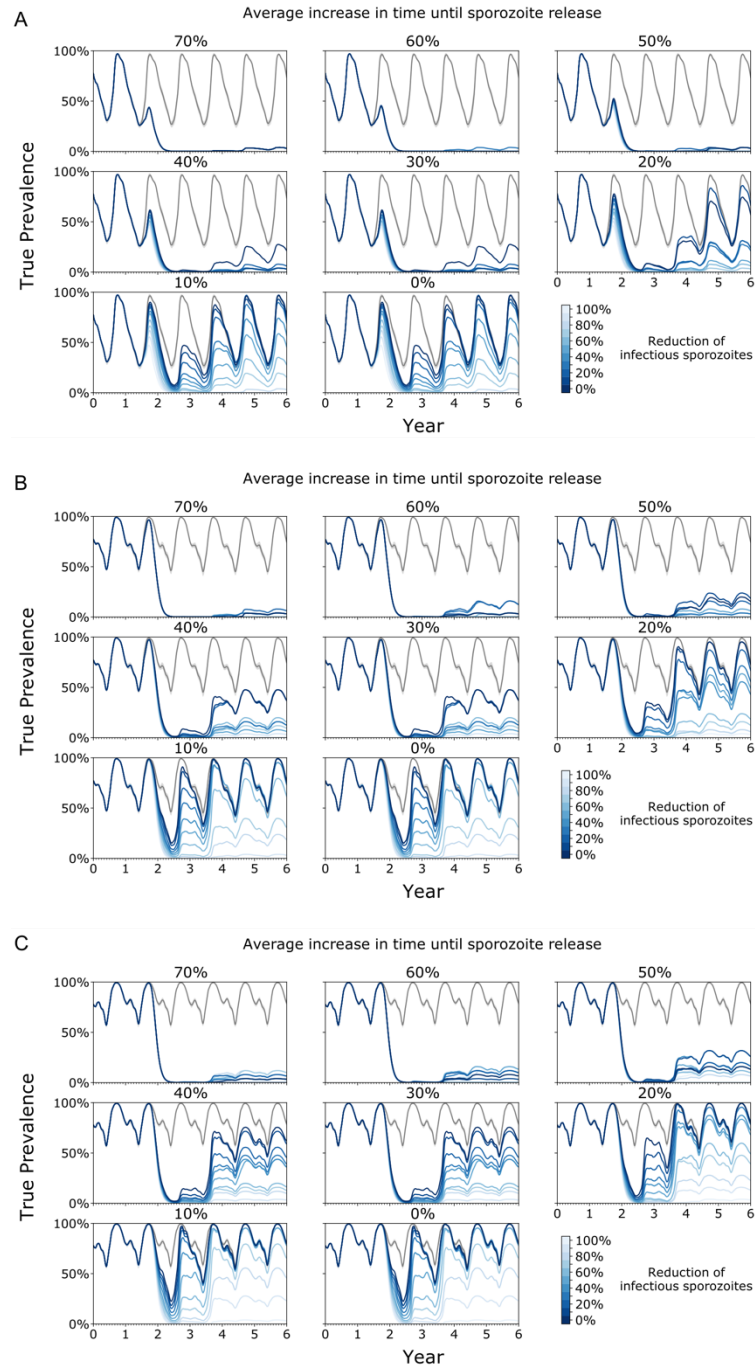


Fig. S7.

The mean time course of true prevalence after 1000 gene drives mosquitoes homozygous for the driver and effector locus are released 6 months into a 6-year simulation. Annual EIR of around 15 (A), 30 (B) and 60 (C) infectious bites per person in an unmitigated scenario. Each panel represents the average increase in time until sporozoites are released while the blue shaded traces each represent a different average reduction in infectious sporozoites. The grey trace represents the unmitigated baseline scenario. There is a temporary reduction in vector numbers when the effector reaches a high frequency because of the fitness costs associated with its expression. This, in conjunction with a reduced lifespan of homozygous females, leads to a temporary reduction in transmission, even when we assume no reduction in infectious sporozoites and no delay in release of sporozoites. This corrects as soon as resistant alleles start to dominate.

GO.ID	Term	Condition	gene counts			p value	
			Annotated	Significant	Expected	elimKS	classicFisher
GO:0046914	transition metal ion binding	6 hours	95	72	59.41	0.004	0.0031
GO:0046872	metal ion binding	6 hours	201	141	125.71	0.106	0.0086
GO:0015318	inorganic m.e. transmembrane transporter activity	20 hours	52	38	27.52	0.00019	0.0018
GO:0015075	ion transmembrane transporter activity	20 hours	59	41	31.23	0.00046	0.0057
GO:0098800	inner mitochondrial membrane protein complex	20 hours	56	39	29.68	0.0021	0.0066
GO:0031966	mitochondrial membrane	20 hours	78	52	41.34	0.4586	0.0073
GO:0005740	mitochondrial envelope	20 hours	80	53	42.4	0.4701	0.0082
GO:0044455	mitochondrial membrane part	20 hours	65	44	34.45	0.384	0.009
GO:0005743	mitochondrial inner membrane	20 hours	72	48	38.16	0.435	0.0099

Table S1.

Enriched GO terms

<i>Fitness & phenotypic parameters</i>				
Locus	Allele combination	Daily mortality (%)	Fecundity (%)	Applied to sex
driver	WT , D		-2.5	M,F
driver	WT , LGF		-10	M,F
driver	D , D		-5	M,F
driver	D , R		-2.5	M,F
driver	D , LGF		-12.5	M,F
driver	R , LGF		-10	M,F
driver	LGF , LGF		-100	M,F
effector	WT , LGF	+10		M,F
effector	E , E	+30	-14	F
effector	E , LGF	+10		M,F
effector	R , LGF	+10		M,F
effector	LGF , LGF	+100		M,F
<i>Gene drive parameters</i>				
Locus	Allele combination	Outcome	Probability	Allele generated
driver	D , <u>WT</u>	Gene Drive (autonomous)	0.97	D
		Unmodified	0.1	WT
		NHEJ to R2	0.1	LGF
		NHEJ to R1	0.1	R
effector	E , <u>WT</u> (+D)	Gene Drive (non-autonomous)	0.97	E
		Unmodified	0.1	WT
		NHEJ to R2	0.1	LGF
		NHEJ to R1	0.1	R

Table S2.

Table of EMOD modelling parameters.

Supplementary file S1. (separate file)

Annotated DNA sequences of transformation vectors pD-MM-CP and pD-Gam1-MM.

Supplementary file S2. (separate file)

DNA oligonucleotide database.